Analyst

ROYAL SOCIETY OF CHEMISTRY

PAPER

View Article Online
View Journal | View Issue

Cite this: *Analyst*, 2021, **146**, 2886

Electrochemical detection of microRNA-21 based on a Au nanoparticle functionalized g-C_3N_4 nanosheet nanohybrid as a sensing platform and a hybridization chain reaction amplification strategy†

Ya Wang, Mengyao Li and Yuzhong Zhang *

Here, a sensitive sandwich-type electrochemical biosensor for microRNA-21 detection was reported. It was based on the use of a Au NP functionalized graphite-like carbon nitride nanosheet (g-C_3N_4 NS) nanohybrid (Au NPs–g-C_3N_4 NS) as a sensing platform and DNA concatemers containing methylene blue (MB) as a signal probe. The signal probe was prepared by using two different single strand DNAs with a complementary sequence (one of them labeled with MB at the 3′ end) to form long concatemers *via* continuous hybridization chain reaction (HCR); thus numerous MB signal molecules were loaded on long concatemers. The biosensor was fabricated following the next step: a thiolated hairpin probe (HP) was first immobilized on the surface of the glassy carbon electrode (GCE) modified with a Au NPs–g-C_3N_4 NS nanohybrid. After it was blocked with MCH, the modified electrode was sequentially hybridized with microRNA-21 and a signal probe, respectively. As a result, a sandwich structure of HP–microRNA–signal probe covered the surface of the modified electrode. Differential pulse voltammetry (DPV) was employed to measure the sensing signal in phosphate buffered solution (0.10 M PBS, pH 7.4). The experimental conditions were optimized such as the hybridization time and the amount of g-C_3N_4 NS. The proposed biosensor exhibited a wide linear response range (1.0 fM to 500 nM) and a low limit of detection (0.33 fM; at S/N = 3) under the optimal conditions. Meanwhile, the biosensor could discriminate single base mismatched microRNA-21, indicating that the biosensor possessed high selectivity.

Received 7th January 2021,
Accepted 26th February 2021

DOI: 10.1039/d1an00029b

rsc.li/analyst

Introduction

As is well known, microRNAs possess short sequences (18–22 nt), low expression levels, and highly similar sequences among family members and play significant regulatory roles in many biological processes such as cellular differentiation and cell apoptosis.[1] The previous literature shows that the dysregulation of the expression of microRNA is correlated to cancer.[2] For example, a higher expression level of microRNA-21 in serum is related to breast and liver cancers.[3] Currently, quantitative reverse transcription polymerase chain reaction (qRT-PCR) and northern blotting are conventional detection methods of microRNA.[4] However, these methods suffer from the need to design primers to label locked nucleic acid (LNA), sample degradation due to RNases and low sensitivity. Hence, it is essential to develop a simple and sensitive detection method of microRNA. To date, various analytical methods of microRNA have emerged including fluorescence,[5] colorimetry,[6] surface plasma resonance (SPR)[7] and electrochemistry.[8–12] Moreover, some reviews related to microRNA assay have been reported.[4,13] Among them, electrochemical methods are fascinating due to their advantages including simplicity, sensitivity and high selectivity. To improve the detection sensitivity, various signal amplifying modes have been reported including nucleases and enzyme-free assisting.[14–22] Enzyme-free amplifying modes including hybridization chain reaction (HCR) and catalyzed hairpin assembly reaction (CHA) have been reported. For instance, Tang's group reported an ultrasensitive electrochemical immunosensor for IgG protein detection based on the HCR amplifying signal;[14] Yuan's group[15] utilized CHA and HCR strategies to realize target recycling and signal amplification for microRNA-155 detection, and the linear response range was from 10 fM to 1 nM with a limit of 3.3 fM; Miao's group[16] adopted a HCR amplifying strategy and Ag NPs as signal tags, which showed that the assay had high sensitivity (the detection limit was 20 aM); Liu's group[17]

College of Chemistry and Materials Science, Anhui Key Laboratory of Chem-Biosensing, Anhui Normal University, Wuhu 241002, People's Republic of China. E-mail: zhyz65@mail.ahnu.edu.cn; Fax: +86553 3869303; Tel: +86 553 3869303

†Electronic supplementary information (ESI) available. See DOI: 10.1039/d1an00029b

employed HCR amplification and CdTe quantum dot (QD) labeled signal strands to electrochemically detect microRNA-2. As a result, the biosensor exhibited a wide linear response range (0.1 fM to 0.1 nM) and a low detection limit (33 aM). Nucleases are used as signal amplification modes to improve the analytical performance. For example, Tang and coworkers employed an exonuclease III-powered DNA walker for CEA detection using a near-infrared light responsive biosensor.[19] Thereafter, the group reported a photoelectrochemical biosensor of kanamycin using a palindromic molecular beacon and polymerase.[20] As a result, the assay showed a wide working range from 50 to 500 fM and a low detection limit of 29 fM. In contrast to enzyme signal amplification, the experiment process of HCR is simple and easy to perform.

Graphite-like carbon nitride (g-C_3N_4) nanosheets (NS), a metal-free semiconductor material, have been recently employed as a good electrochemiluminescence (ECL) emitter. However, they have a low electron transfer rate and low conductivity to restrict their application in the sensing field. In order to overcome the defects, metal nanoparticles (*e.g.* Au NPs) are often used to form a g-C_3N_4 NS–metal nanoparticle hybrid. The nanohybrid can clearly improve the catalysis and ECL performance.[23,24] Inspired by the literature, the Au NPs–g-C_3N_4 NS hybrid was employed as a sensing base material in the present work to improve the sensing performance. HCR was used to form a signal probe to improve the sensing performance. In contrast to other HCR amplification methods, this method has the following advantage: the signal probe is prepared in advance *via* HCR; thus long DNA concatemers can be easily obtained and verified. The experimental conditions are gentle. In terms of design, a thiolated hairpin probe (HP) was used as the capture probe and first immobilized on the surface of Au NPs–g-C_3N_4 NS/GCE; only after hybridization with microRNA-21 did the hairpin structure open up, and then the signal probe was incubated with microRNA-21-HP/Au NPs–g-C_3N_4 NS/GCE, resulting in a sandwich structure of signal probe–microRNA–HP formed on the surface of Au NPs–g-C_3N_4 NS, and the electrochemical signal was clearly increased. As a result, the microRNA biosensor exhibited a wide linear response range (1.0 fM to 500 nM) and a low limit of detection (0.33 fM).

Experimental

Chemicals and reagents

Chloroauric acid ($HAuCl_4 \cdot 4H_2O$) and tris(hydroxymethyl)aminomethane (Tris) were purchased from Sinopharm Chemical Reagent Co., Ltd. Melamine, 6-mercapto-1-hexanol (MCH), sodium borohydride ($NaBH_4$), trisodium citrate and various oligonucleotides were synthesized by Sangon Inc (Shanghai, China), and the sequences are as follows (in the hairpin probe, the loop is italicized and the sticky ends are underlined):

Hairpin probe (HP): 5′-HS-SH-$(CH_2)_6$-CCG GGT *TCA ACA TCA GTC TGA TAA GCT* AAC CCG G-3′

Signal sequence 1 (P_1): 5′-CCG TTC CGA GTT GTG ACC CGG CTA CAT GGA-MB-3′

Auxiliary sequence 2 (P_2): 5′-CAC AAC TCG GAA CGG TCC ATG TAG CCG GGT-3′

MicroRNA-21: 5′-UAG CUU AUC AGA CUG AUG UUG A-3′

Single base mismatched sequence (M_1): 5′-UAG AUU AUC AGA CUG AUG UUG A-3′

(M_2): 5′-UAG CUU AUC ACA CUG AUG UUG A-3′

(M_3): 5′-UAG CUU AUC AGA CUG GUG UUG A-3′

Noncomplementary sequence: 5′-GUA AGG CAU CUG ACC GAA GGA A-3′

The following buffered solutions were employed throughout the experiment: TE buffer solution (10 mM Tris-HCl + 1.0 mM EDTA, pH 7.4) was used for dissolving various oligonucleotides. 0.10 M PBS containing 0.10 M NaCl (pH 7.4) was employed as the detection solution. 0.01 M PBS containing 0.10 M NaCl (pH 7.4) was used as the hybridization solution. $[Fe(CN)_6]^{3-/4-}$ was used as the redox probe of cyclic voltammetry (CV) or electrochemical impedance spectroscopy (EIS) to investigate the assembling process of the biosensor. All solutions prepared were treated in advance with diethyl pyrocarbonate (DEPC)-treated water (RNase-free) (Sangon Inc, Shanghai) and twice-distilled water was used in this study. The serum samples were kindly provided by Anhui Normal University Hospital, Wuhu, and all experiments were performed in accordance with the relevant laws and institutional guidelines of China, and approved by the ethics committee at Anhui Normal University. Informed consents were obtained from human participants of this study.

Apparatus

A CHI650C electrochemical analyzer (Chenhua, Shanghai) with a three electrode system was employed for various electrochemical measurements. A bare or modified glassy carbon electrode (GCE, Ø = 3.0 mm) was used as the working electrode, a platinum wire was used as the auxiliary electrode and a saturated calomel electrode (SCE) was used as the reference electrode. All potentials were referenced to the SCE. Scanning electron microscopy (SEM) (Hitachi S-8100, Japan) was used to obtain the morphologies of g-C_3N_4 NS and Au NPs–g-C_3N_4 NS. A fusion FX7 EDGE imaging system (VILBER LOURMAT, Co, France) was used for the gel electrophoresis experiment.

Synthesis of g-C_3N_4 NS and preparation of the Au NPs–g-C_3N_4 NS hybrid

The bulk g-C_3N_4 material was prepared following the previous literature.[24,25] In detail, 10 g of melamine was placed in a crucible, and then heated at 600 °C for 2 h at a heating rate of 3 °C min^{-1}; then it was cooled to room temperature at a rate of 3 °C min^{-1}. As a result, a yellow powder was obtained. Subsequently, 30 mg bulk g-C_3N_4 powder was ultrasonically agitated for 16 h and dispersed in 50 mL water. The final formed suspension was centrifuged at 6000 rpm to remove the residual unexfoliated g-C_3N_4 NS, and the mass concentration of the g-C_3N_4 NS suspension was calculated by weighing the powder dried from a certain volume of the suspension. The concentration of g-C_3N_4 NS was 0.01 mg mL^{-1}.

Au NPs–g-C_3N_4 NS was prepared following the next procedure.[24] In brief, 300 μL of 0.01 M $HAuCl_4$ solution was added slowly to 50 mL of 0.01 mg mL^{-1} g-C_3N_4 NS suspension under stirring and ultrasonic agitation for 30 min at room temperature. Afterward, 1.0 mL of 0.50 mg mL^{-1} $NaBH_4$ (fresh preparation) was added quickly to the above suspension and stirred for 20 min in an ice bath. Finally, 1.0 mL of 1.5 mg mL^{-1} sodium citrate was added to the above suspension under stirring, and the stirring process was continued for 30 min. After centrifugal separation, the obtained product was redispersed in water to obtain 0.05 mg mL^{-1} of Au NPs–g-C_3N_4 NS.

Preparation of the signal probe

The signal probe was obtained according to our previous report:[26] briefly, 100 μL of 2.0 μM signal sequence (P_1) was incubated with 100 μL of 2.0 μM auxiliary sequence (P_2) for 2.5 h at 37 °C, resulting in a continuous hybridization reaction between P_1 and P_2 to form long DNA concatemers during this process. A gel electrophoresis experiment verified the formation of DNA concatemers.

Fabrication of the microRNA sensor

The sensing mechanism is shown in Scheme 1. The bare GCE was first polished with an alumina slurry (0.3 μm, 0.05 μm) and washed ultrasonically for three minutes (water, ethanol), respectively. Then, 5.0 μL of 0.05 mg mL^{-1} Au–g-C_3N_4 NS was injected on the surface of the GCE and naturally dried. Subsequently, 16.0 μL of 1.0 μM HP was dropped onto the surface of Au–g-C_3N_4 NS and kept for 12 h in a refrigerator. The modified electrode was then incubated with MCH (1%) for 1 h to block the active sites of the electrode surface. The electrode was denoted as MCH/HP/Au–g-C_3N_4 NS/GCE. Subsequently, 10.0 μL of various concentrations of microRNA-21 or serum sample was dropped on the surface of MCH/HP/Au–g-C_3N_4 NS/GCE and incubated for 80 min at 37 °C. Finally, 10.0 μL of 1.0 μM signal probe was injected on the surface of microRNA-21/MCH/HP/Au–g-C_3N_4 NS/GCE, and incubated for 60 min; thus the sandwich structure of HP–microRNA-21–signal probe was formed. The fabricated microRNA biosensor was rinsed and transferred to an electrolytic cell for measurement. As a result, a sensitive sensing signal was obtained and is shown in Scheme 1 (right).

Electrochemical measurements

Electrochemical measurements were performed in an electrolytic cell with a three electrode system. The characteristics of the assembling process of the biosensor was performed step by step by cyclic voltammetry (CV) or the electrochemical impedance spectra (EIS) technique. Differential pulse voltammetry (DPV) was performed in 5.0 mL of 0.10 M PBS (pH 7.4). Before the experiment, high-purity nitrogen (N_2) was passed into the solution for 10 min and the N_2 atmosphere was maintained during the measurement. The DPV parameters are listed as follows: potential range, −0.6 V to 0 V; pulse amplitude, 0.05 V; pulse width, 0.08 s; sample interval, 0.002 s.

EIS curves were obtained in 0.10 M PBS (pH 7.4) containing 5.0 mM $[Fe(CN)_6]^{3-/4-}$ at a formal potential of 0.18 V (*vs.* SCE). The other parameters are as follows: frequency range, 0.1 to 100 kHz; AC potential amplitude, 5 mV.

Results and discussion

Choice of materials

According to the literature, g-C_3N_4 NS has a similar structure to that of graphene and weak electron transfer ability, and Au NPs possess good conductivity and biocompatibility. Therefore, the Au NPs–g-C_3N_4 NS nanohybrid provides better conductivity and has been used in the sensing field for improving the sensing performance. In this study, we employed Au NPs or Au NPs–g-C_3N_4 NS as a sensing base material respectively (the other conditions were the same); the

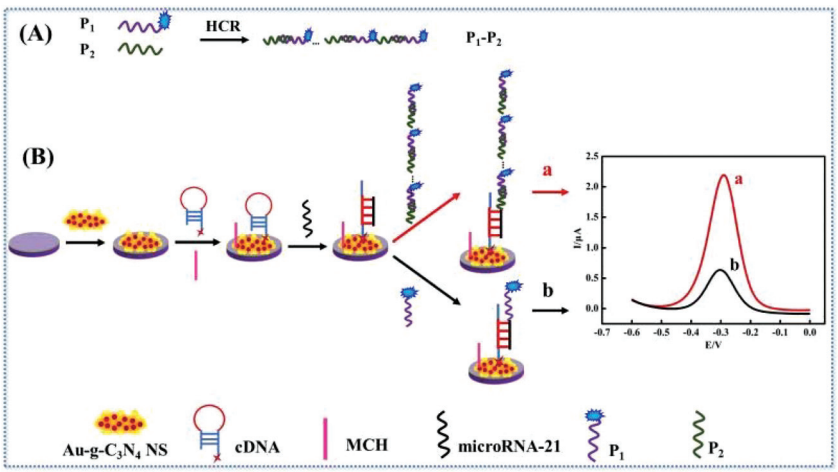

Scheme 1 Schematic illustration of the protocol of the microRNA biosensor. (A) Preparation of the signal probe. (B) The step by step assembling process of the microRNA sensor.

response signal obtained was clearly different when it was employed to detect the same concentration of microRNA. The signal intensity of the Au NPs–g-C_3N_4 NS base material was 2.6-fold higher than that of the Au NP base material (see Fig. S1†), indicating that Au NPs–g-C_3N_4 NS as the base material improves the electrode surface area and the immobilization amount of HP clearly. Furthermore, the sensing performance was clearly improved.

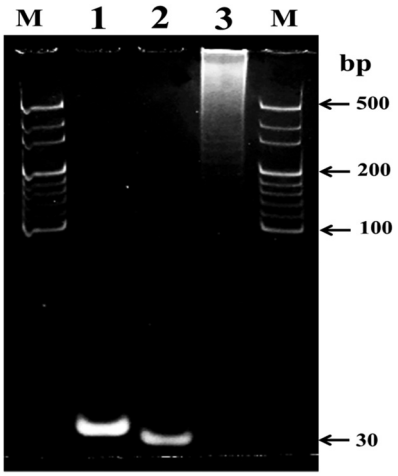

Fig. 1 Gel electrophoresis image obtained under various conditions. Lane M, DNA marker; lane 1, 1.0 μM P_1; lane 2, 1.0 μM P_2 and lane 3, 1.0 μM P_1 + 1.0 μM P_2.

Characterization of the signal probe

In order to investigate the formation of the signal probe, a gel electrophoresis experiment was performed. In this work, two different single strand DNAs (P_1, P_2) were specifically designed. 15 bases (underlined) of P_1 are complementary with 15 bases of P_2 (underlined), and other 15 bases are complementary with 15 bases of P_2 (not underlined). So, when P_1 hybridizes with P_2 in a hybridization solution, longer DNA concatemers are formed *via* continuous HCR. Fig. 1 shows various electrophoretic bands of different DNA samples. It can be seen that the base of DNA concatemers is more than 500 bp (see lane 4), indicating the formation of the signal probe.

Electrochemical investigation

g-C_3N_4 NS and Au NPs–g-C_3N_4 NS were first investigated with SEM (see Fig. 2). It can be seen that g-C_3N_4 NS presents a thin wrinkled structure similar to that of graphene (see Fig. 2A) and Au NPs were uniformly dispersed on its surface (Fig. 2B) with an average diameter of about 5 nm (Fig. 2C). Fig. 2D shows the EDX curves of g-C_3N_4 NS and Au NPs–g-C_3N_4 NS; it can be seen that the peaks of C, N and Au appeared, indicating that g-C_3N_4 NS and Au NPs–g-C_3N_4 NS were successfully prepared. The effective surface area of the Au NPs–g-C_3N_4 NS modified electrode was 0.197 cm^2, which was higher than that of the bare electrode (0.13 cm^2) according to the Randles–Sevcik equation and using $[Fe(CN)_6]^{3-/4-}$ as the redox probe (i_p = 2.69 × 10^5 $An^{3/2}$ $D_0^{1/2}$ $V^{1/2}$ C_0, here, D_0 = 7.6 × 10^{-6} cm^2 s^{-1}, n = 1, C_0 = 1.0 mM). Fig. 3A shows the CVs of $[Fe(CN)_6]^{3-/4-}$ at

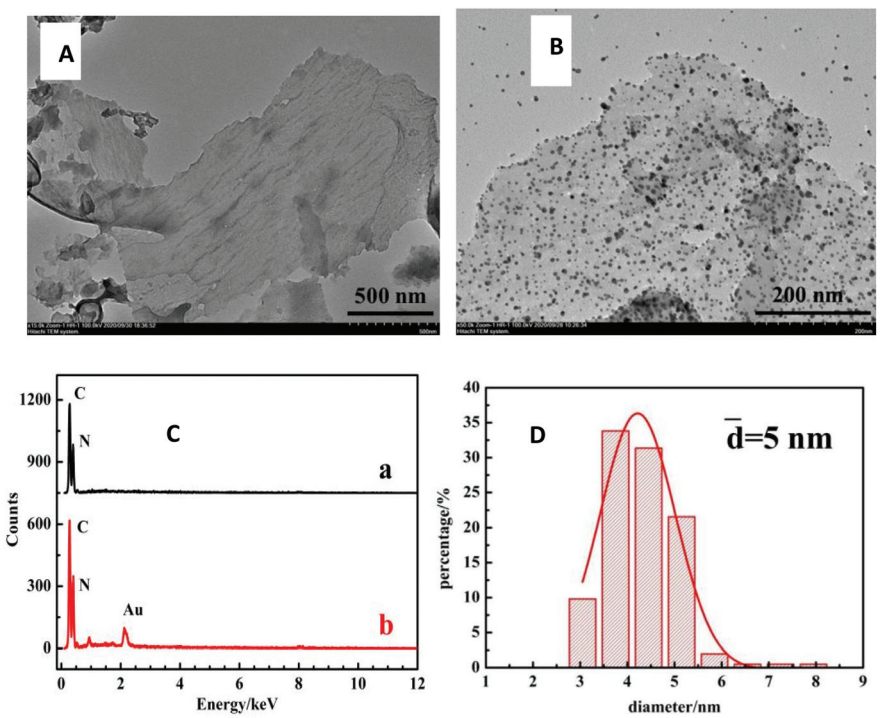

Fig. 2 (A) TEM images of g-C_3N_4 NS and (B) Au NPs–g-C_3N_4 NS; (C) EDX curves of g-C_3N_4 NS (a) and Au NPs–g-C_3N_4 NS (b); (D) size distribution of Au NPs.

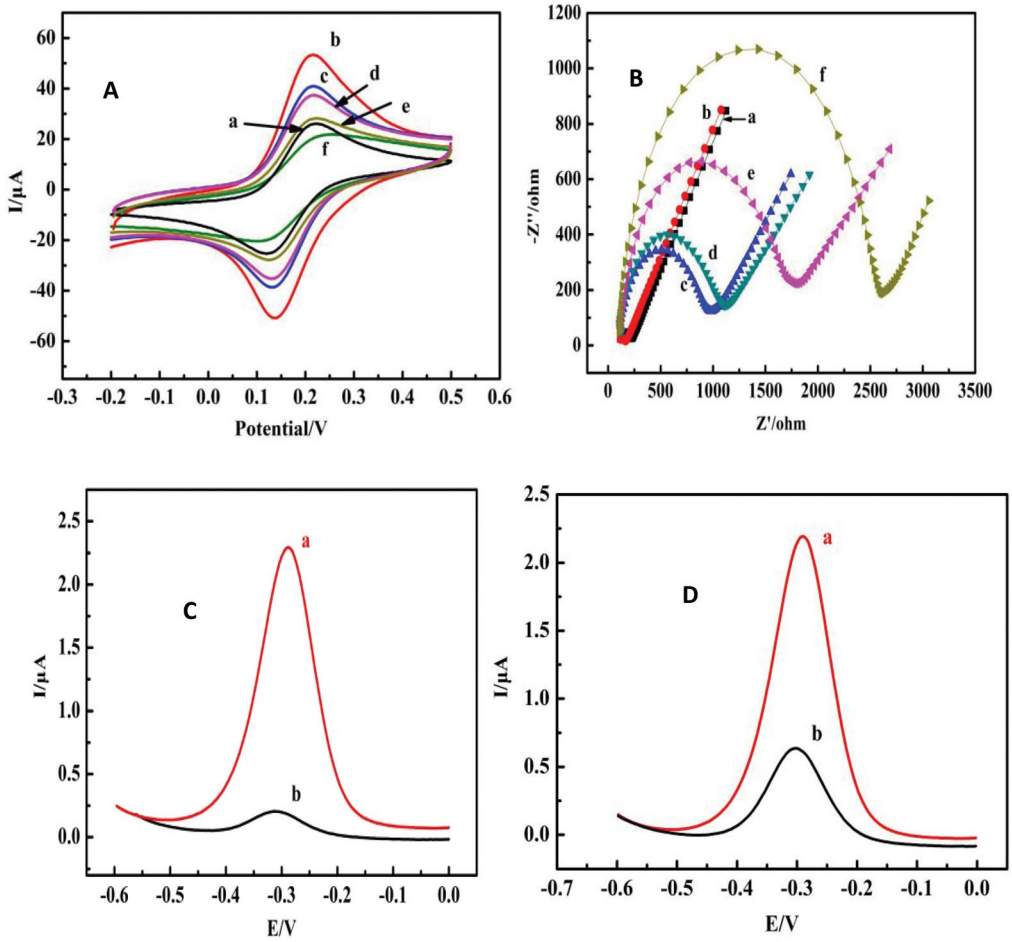

Fig. 3 (A) CVs of 1.0 mM $[Fe(CN)_6]^{3-/4-}$ recorded at different assembling steps of the microRNA biosensor, and (B) EIS curves of 5.0 mM $[Fe(CN)_6]^{3-/4-}$ at the different assembling steps of the microRNA biosensor. Curves of (a) GCE; (b) Au NPs–g-C_3N_4 NS/GCE; (c) HP/Au NPs–g-C_3N_4 NS/GCE; (d) MCH/HP/Au NPs–g-C_3N_4 NS/GCE; (e) microRNA-21/MCH/HP/Au NPs–g-C_3N_4 NS/GCE; and (f) signal probe/microRNA-21/MCH/HP/Au NPs–g-C_3N_4 NS/GCE. (C) DPV responses of the biosensor in 0.10 M pH 7.4 PBS containing 0.10 M NaCl recorded in the absence (b) and presence of microRNA-21. Conditions: $C_{microRNA}$ = 1.0 pM. $C_{signal\ probe}$ = 1.0 μM. (D) DPV responses of the microRNA sensor in the presence of a short sequence labeled with MB (black) and long DNA concatemers (red) containing MB as the signal probe.

different assembling steps of the biosensor. After Au NPs–g-C_3N_4 NS was coated (curve b), the peak current was clearly increased in contrast to the bare GCE (curve a). Along with the HP probe, MCH, microRNA and the signal probe were sequentially assembled on the surface of Au NPs–g-C_3N_4 NS; the negatively charged probes (HP, microRNA and the signal probe) repel the negatively charged $[Fe(CN)_6]^{3-/4-}$, leading to the gradual decrease of the peak currents of $[Fe(CN)_6]^{3-/4-}$. Fig. 3B shows the EIS curves at different assembling steps. The electrode modified with Au NPs–g-C_3N_4 NS exhibited an almost straight line (curve b). Along with HP and MCH assembled on the electrode surface, a small semicircle was observed in the EIS curves, and the diameter of the semicircle was increased. Subsequently, the target microRNA and the signal probe were assembled on the electrode surface, respectively. The semicircle was continuously enlarged. When the modified electrode was transferred to the electrolytic cell containing 0.1 M pH 7.4 PBS, a sensitive DPV signal was obtained at a peak potential of about −0.33 V (*vs.* SCE) corresponding to MB, indicating that the assembling procedure was successful (curve a in Fig. 3C). Meanwhile, a contrast test was performed in the absence of microRNA-21 (the other assembling steps were the same); a weak signal was obtained in the DPV curves due to weak absorption of the signal probe (curve b in Fig. 3C). So, washing was needed after each assembling step.

Optimization of experimental conditions

In order to obtain a higher sensitivity, some experiment conditions were optimized such as solution pH, amount of Au–g-C_3N_4 NS and HP, and incubation time (P_1–P_2; HP and microRNA; microRNA and signal probe). The experimental results obtained are presented in the ESI (Fig. S2†). As shown in Fig. S2,† the following experimental conditions were the most suitable: pH value, 7.4; incubation time of P_1–P_2, 150 min; incubation time of HP–microRNA, 80 min; hybridization time of microRNA–signal probe, 60 min. The amount of 0.05 mg mL^{-1} Au–g-C_3N_4 NS and 1.0 μM HP was 10 μL and 16 μL, respectively.

Signal amplification

In this work, two different signal probes were employed for investigation: one was a short strand probe labeled with MB (P_1) and the other was long DNA concatemers from P_1–P_2 continuous hybridization reaction; 1.0 pM of microRNA-21 was used. The electrochemical responses obtained are shown in Fig. 3D. The larger signal was obtained in the presence of long DNA concatemers, indicating that HCR amplifies the response signal. The reason for this was that long DNA concatemers loaded lots of MB signal molecules.

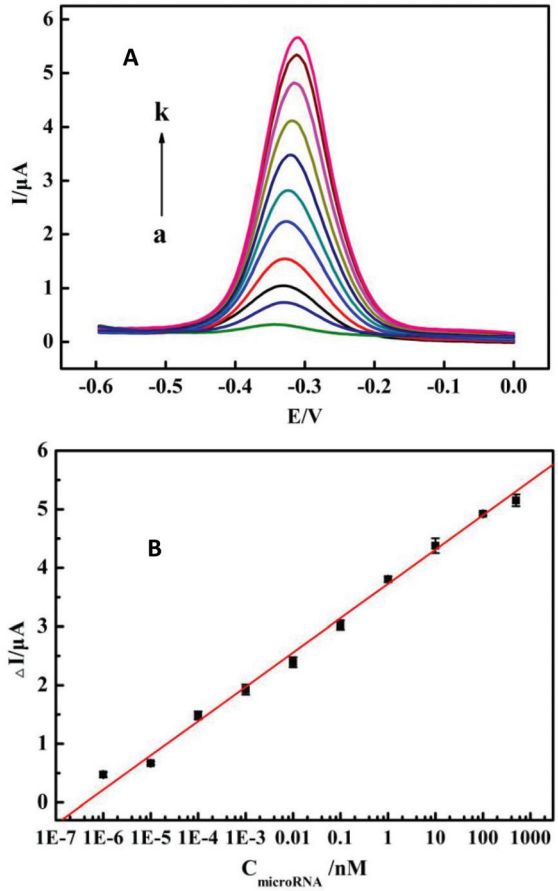

Fig. 4 (A) DPV responses of the microRNA sensor corresponding to various microRNA concentrations in 0.10 M pH 7.4 PBS containing 0.10 M NaCl: (a) 0.0 fM; (b) 1.0 fM; (c) 10.0 fM; (d) 100 fM; (e) 1.0 pM; (f) 10.0 pM; (g) 100 pM; (h) 1.0 nM; (i) 10.0 nM; (j) 100 nM; and (k) 500 nM. (B) Calibration plots of peak current *vs.* logarithm of the microRNA concentration.

Analytical performance

The analytical performance of the biosensor was evaluated using a series of concentrations of microRNA-21. The peak currents at a peak potential of about −0.33 V (*vs.* SCE) increased as the concentrations of microRNA-21 increased (Fig. 4A), and a good calibration curve was obtained from 1.0 fM to 500 nM (see Fig. 4B) with a detection limit of 0.33 fM (at S/N = 3). The linear regression equation was ΔI (μA) = 0.585 lg C (nM) + 1.972 (R^2 = 0.9980). In contrast to the previous reported work (see Table 1), the analytical performance of the biosensor was good from the viewpoints of the linear range and detection limit which can meet the requirements of real sample analysis.

Selectivity, reproducibility and stability

In this investigation, we selected a single base mismatched (C, G, A) and noncomplementary sequence with microRNA-21 for selectivity evaluation. The results are shown in Fig. 5 with histograms (inset DPV curves). From Fig. 5, it can be seen that the signal intensity corresponding to microRNA-21 was the largest, and signal intensities corresponding to single base mismatched sequences (B, C, D) was lower, and only obtain about 23% that of microRNA-21, and signal intensity corresponding to the noncomplementary sequence was the lowest which was the same as that of the background signal (lack of target) (about 5% signal intensity of microRNA-21). These fact indicated that the microRNA sensor possesses good selectivity which can discriminate single base mismatched target sequences.

The reproducibility of the sensor was examined using four sensors independently prepared under the same conditions to detect 1.0 pM microRNA-21 and the signal intensities were recorded. All biosensors exhibit similar electrochemical

Table 1 Analytical performance of various electrochemical microRNA biosensors

Detection method	Used material	Analytical time	Target microRNA	Linear range	Detection limit	Ref.
Electrochemical	WO_3–GO	2.5 h	microRNA-21	0.1 fM–100 pM	0.05 fM	8
Electrochemical	$MoSe_2$–Au NPs	3.5 h	microRNA-21	10 fM–1 nM	0.17 fM	10
Electrochemical	Au NPs–GO	4 h	microRNA-155	10 fM–1 nM	3.3 fM	15
Electrochemical	HCR and Au NPs	4 h	microRNA-21	10 aM–100 pM	2 aM	16
Electrochemical	HCR + CdTe QDs	3.5 h	microRNA-21	0.1 fM–0.1 nM	33 aM	17
Electrochemical	CHA–RCA	1.5 h	microRNA-21	0.5 pM–12.5 nM	290 fM	27
Electrochemical	DA–Au NPs	1.5 h	microRNA-21	0.1 pM–10 pM	45 fM	28
Electrochemical	Au–PtBNPs	0.5 h	microRNA-21	1 fM–1.0 μM	1 fM	29
Electrochemical	Enzyme and molecular beacon	1.5 h	microRNA-222	50 pM–10 nM	40 pM	30
Electrochemical	Fe_3O_4 NPs–HCR	5.5 h	microRNA-21	1 fM–1 nM	0.28 fM	31
Electrochemical	Ag NPs	1.5 h	microRNA-21	0.1 fM–50 fM	20 aM	32
Electrochemical	Au NPs–g-C_3N_4 NS + HCR	2.2 h	microRNA-21	1.0 fM–500 nM	33 aM	This work

QDs: graphene quantum dots; HCR: hybridization chain reaction; NPs: nanoparticles; DA–Au NPs: dopamine (DA)–capped Au NPs; Au–PtBNPs: gold platinum bimetallic nanoparticles.

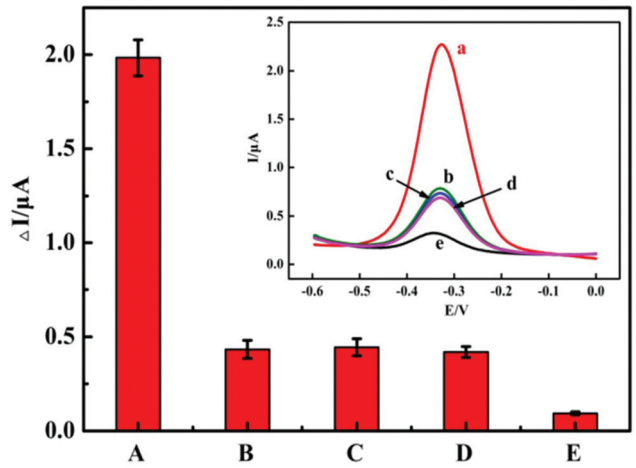

Fig. 5 Selectivity of the biosenor for microRNA-21. (A) microRNA-21; (B) single-base A mismatched sequence; (C) single-base C mismatched sequence; (D) single-base G mismatched sequence; and (E) noncomplementary sequence. Inset: DPVs of the biosensor corresponding to different sequence microRNA (microRNA-21) (curve a), single-base mismatched sequence (curves b, c, and d) and noncomplementary sequence (curve e). The concentration of the different sequences was 1.0 pM.

responses and the relative standard deviation was 3.5%, indicating that the reproducibility was acceptable. The stability of the biosensor was evaluated by recording the signal value for a week (one time per day) in the detection solution. The response values of the sensor were relatively stable, and the sensor on the seventh day could retain 92.9% of its initial response, indicating that the stability was acceptable.

Analytical application

In order to investigate the application of the microRNA sensor in clinical samples, recovery experiments were performed by spiking various concentrations of microRNA-21 (1.0 and 10.0 pM) into healthy human serum samples (the serum samples were first centrifuged, and the upper solution was collected for the detection sample). The DPV technique was employed to record the response signal of the biosensor; the serum samples shows a weak signal in which the signal intensity is almost zero. When microRNA-21 was added in the serum samples, the signal intensity was clearly increased (b, c) (see Fig. S3†) and the content of the sample was calculated using working curves, and the results are shown in Table 2. The recoveries were within 96.5%–103.6% and RSDs were within 2.16%–4.17%, indicating that the microRNA sensor can be applied to serum sample analysis.

Table 2 Recovery results obtained in the serum sample with this method (n = 3)

Samples	Added (pM)	Detected (pM)	Recovery (%)	RSD (%)
1	1	$1.06^{a} \pm 0.27^{b}$	100.4%	4.17
	10	$9.65^{a} \pm 0.38^{b}$	103.6%	3.52
2	1	$0.95^{a} \pm 0.16^{b}$	97.8%	2.16
	10	$9.66^{a} \pm 0.49^{b}$	96.5%	2.39

[a] Average value of three determination results. [b] Standard deviation.

Conclusions

A sensitive electrochemical biosensor for microRNA-21 detection was fabricated. A g-C_3N_4 NS–Au NPs nanohybrid was used as the sensing platform and the hybridization chain reaction amplified the response signal. The sensor displays good sensing performance (wider response range and low limit of detection). Furthermore, the microRNA biosensor can be applied to the detection of microRNA in serum.

Conflicts of interest

There are no conflicts to declare.

Acknowledgements

This work was financially supported by the Natural Science Foundation of Education Department of Anhui Province (no. KJ2016A848).

References

1 K. J. Png, N. Halberg, M. Yoshida and S. F. Tavazoie, *Nature*, 2012, **481**, 190–194.
2 S. Volinia, G. A. Calin, C. G. Liu, S. Ambs, A. Cimmion, F. Petrocca, R. Visone, M. Iorio, C. Roldo, M. Ferracin, R. L. Prueitt, N. Yanaihara, G. Lanza, A. Scarpa, A. Vecchione, M. Negrini, C. C. Harris and C. M. Croce, *Proc. Natl. Acad. Sci. U. S. A.*, 2006, **103**, 2257–2261.
3 F. Wang, Z. Zheng, J. Guo and X. Ding, *Gynecol. Oncol.*, 2010, **119**, 586–593.
4 T. Kilic, A. Erdem, M. Ozsoz and S. Carrara, *Biosens. Bioelectron.*, 2018, **99**, 525–546.
5 L. Yang, C. H. Liu, W. Ren and Z. P. Li, *ACS Appl. Mater. Interfaces*, 2012, **4**, 6450–6453.
6 Y. L. Zhang, Z. P. Li, Y. Q. Cheng and X. C. Lv, *Chem. Commun.*, 2009, **22**, 3172–3174.
7 S. P. Fang, H. J. Lee, A. W. Wark and R. M. Corn, *J. Am. Chem. Soc.*, 2006, **128**, 14044–14046.
8 H. L. Shuai, K. J. Huang, L. L. Xing and Y. X. Chen, *Biosens. Bioelectron.*, 2016, **86**, 337–345.
9 Z. Y. Wang, L. Si, J. C. Bao and Z. H. Dai, *Chem. Commun.*, 2015, **51**, 6305–6307.
10 Y. H. Wang, K. J. Huang, X. Wu, Y. Y. Ma, D. L. Song, C. Y. Du and S. H. Chang, *J. Mater. Chem. B*, 2018, **6**, 2134–2142.
11 Y. H. Liao, R. Huang, Z. K. Ma, Y. X. Wu, X. M. Zhou and D. Xiung, *Anal. Chem.*, 2014, **86**, 4596–4604.

12 W. F. Lv, J. M. Zhao, B. Li, W. Ma, J. M. Liu, Z. X. Wu, W. Wang, X. H. Yan and L. Zheng, *Biosens. Bioelectron.*, 2016, **83**, 250–255.
13 Y. H. Wang, L. L. He, K. J. Huang, Y. X. Chen, S. Y. Wang, Z. H. Liu and D. Li, *Analyst*, 2019, **144**, 2849–2866.
14 B. Zhang, B. Q. Liu, D. P. Tang, R. Niessner, G. N. Chen and D. Knopp, *Anal. Chem.*, 2012, **84**, 5392–5399.
15 X. Y. Wu, Y. Q. Chai, R. Yuan, Y. Zhuo and Y. Chen, *Sens. Actuators, B*, 2014, **203**, 296–302.
16 P. Miao, Y. G. Tang and J. Yin, *Chem. Commun.*, 2015, **51**, 15603–15740.
17 H. Y. Liu, X. Q. Bei, Q. T. Xia, Y. Fu, S. Zhang, M. C. Liu, K. Fan, M. Z. Zhang and Y. Yang, *Microchim. Acta*, 2016, **183**, 297–304.
18 J. Shu and D. P. Tang, *Anal. Chem.*, 2020, **92**, 363–377.
19 S. Z. Lv, K. Y. Zhang, L. Zhu and D. P. Tang, *Anal. Chem.*, 2020, **92**, 1470–1476.
20 R. J. Zeng, Z. B. Luo, L. S. Su, L. J. Zhang, D. P. Tang, R. Niessner and D. Knopp, *Anal. Chem.*, 2019, **91**, 2447–2454.
21 Z. L. Ge, M. H. Lin, P. Wang, H. Pei, J. Yan, J. Y. Shi, Q. Huang, D. N. He, C. H. Fan and X. L. Zuo, *Anal. Chem.*, 2014, **86**, 2124–2130.
22 F. Z. Xu, H. Shi, X. X. He, K. M. Wang, D. G. He, Q. P. Guo, Z. H. Qing, L. A. Yan, X. S. Ye, D. Li and J. L. Tang, *Anal. Chem.*, 2014, **86**, 6976–6982.
23 J. Zhu, P. Xiao, H. Li and S. A. Carabineiro, *ACS Appl. Mater. Interfaces*, 2014, **6**, 16449–16465.
24 Q. M. Feng, Y. Z. Shen, M. X. Li, Z. L. Zhang, W. Zhao, J. J. Xu and H. Y. Chen, *Anal. Chem.*, 2016, **88**, 937–944.
25 J. Tian, Q. Liu, A. M. Asiri, A. O. Aiyoubi and X. Sun, *Anal. Chem.*, 2013, **85**, 5595–5599.
26 J. J. Zhang, W. J. Zhang, J. J. Guo, J. C. Wang and Y. Z. Zhang, *Anal. Biochem.*, 2017, **539**, 1–7.
27 Q. Li, F. P. Zeng, N. L. Yu and J. Liang, *Analyst*, 2018, **143**, 2304–2309.
28 N. Xia, L. P. Zhang, G. F. Wang, Q. Q. Feng and L. Liu, *Biosens. Bioelectron.*, 2013, **47**, 461–466.
29 A. Bharti, N. Agnihotri and N. Prabhakar, *Microchim. Acta*, 2019, **186**, 185–196.
30 M. G. Wang, B. Shen, R. Yuan, W. Cheng, H. B. Xu and S. J. Ding, *J. Electroanal. Chem.*, 2015, **756**, 147–152.
31 Y. H. Yuan, Y. D. Wu, B. Z. Chi, S. H. Wen, R. P. Liang and J. D. Qiu, *Biosens. Bioelectron.*, 2017, **97**, 325–331.
32 L. L. Liu, Y. Chang, N. Xia, P. Z. Peng, L. P. Zhang, M. G. Jiang, J. B. Zhang and L. Liu, *Biosens. Bioelectron.*, 2017, **94**, 235–242.